Electronic Supplementary Material (ESI) for Journal of Materials Chemistry C

Electronic Supplementary Information

for

Highly efficient iridium(III) phosphors with phenoxy-substituted ligands and their high-performance OLEDs fabricated by both vacuum deposition and solution processing methods

Guiping Tan,[a,b] Shuming Chen,[c] Ning Sun,[d] Yanhu Li,[e] Daniel Fortin,[f] Wai-Yeung Wong,*[a] Hoi-Sing Kwok,*[c] Dongge Ma,*[d] Hongbin Wu,*[e] Lixiang Wang,[d] and Pierre D. Harvey*[f]

Table S1 Selected bond lengths and angles of **1**.

Selected Bond	Bond Length (Å)	Selected Bond	Bond Length (Å)
Ir(1)-C(8)	2.004(3)	Ir(1)-N(1)	2.126(3)
Ir(1)-C(26)	2.021(3)	Ir(1)-N(2)	2.135(3)
Ir(1)-C(44)	2.003(3)	Ir(1)-N(3)	2.139(3)
Selected Angle	**Bond Angle (^{o})**	**Selected Angle**	**Bond Angle (^{o})**
C(44)-Ir(1)-C(8)	94.0(1)	C(26)-Ir(1)-N(2)	79.1(1)
C(44)-Ir(1)-C(26)	94.5(1)	N(1)-Ir(1)-N(2)	92.9(1)
C(8)-Ir(1)-C(26)	97.6(1)	C(44)-Ir(1)-N(3)	79.3(1)
C(44)-Ir(1)-N(1)	93.6(1)	C(8)-Ir(1)-N(3)	171.1(1)
C(8)-Ir(1)-N(1)	79.4(1)	C(26)-Ir(1)-N(3)	88.8(1)
C(26)-Ir(1)-N(1)	171.6(1)	N(1)-Ir(1)-N(3)	95.2(1)
C(44)-Ir(1)-N(2)	173.4(1)	N(2)-Ir(1)-N(3)	98.9(1)
C(8)-Ir(1)-N(2)	88.4(1)		

Table S2 Selected bond lengths and angles of **2**.

Selected Bond	Bond Length (Å)	Selected Bond	Bond Length (Å)
Ir(1)-C(9)	1.992(4)	Ir(1)-C(27)	1.992(4)
Ir(1)-N(1)	2.034(3)	Ir(1)-N(2)	2.042(3)
Ir(1)-O(3)	2.142(3)	Ir(1)-O(4)	2.163(3)
Selected Angle	**Bond Angle (^{o})**	**Selected Angle**	**Bond Angle (^{o})**
C(27)-Ir(1)-C(9)	93.7(2)	N(1)-Ir(1)-O(3)	89.9(1)
C(27)-Ir(1)-N(1)	94.0(1)	N(2)-Ir(1)-O(3)	95.1(1)
C(9)-Ir(1)-N(1)	81.4(1)	C(27)-Ir(1)-O(4)	90.3(1)
C(27)-Ir(1)-N(2)	81.1(1)	C(9)-Ir(1)-O(4)	174.4(1)
C(9)-Ir(1)-N(2)	96.4(1)	N(1)-Ir(1)-O(4)	94.4(1)
N(1)-Ir(1)-N(2)	174.5(1)	N(2)-Ir(1)-O(4)	88.2(1)
C(27)-Ir(1)-O(3)	175.8(1)	O(3)-Ir(1)-O(4)	87.7(1)
C(9)-Ir(1)-O(3)	88.7(1)		

Table S3 Computed electronic density of the frontier orbitals for **1** (up) and **2** (bottom).

Atom	% of electronic density	
	HOMO	LUMO
C	71.74	75.62
H	4.34	6.05
O	4.98	3.27
N	6.28	12.59
Ir	12.70	2.48

Atom	% of electronic density	
	HOMO	LUMO
C	65.15	71.57
H	4.97	6.06
O	9.21	5.64
N	4.80	11.31
Ir	15.88	5.42

Table S4 Calculated transition energy, position of the 0-0 peaks, oscillator strength (f) and major contributions for the 20 first transitions for **1** (top) and **2** (below).

No.	ν(cm^{-1})	λ(nm)	f	Major contributions (%)
1	23990	416.8	0.025	HOMO→LUMO (94)
2	24279	411.8	0.010	HOMO→L+1 (94)
3	24341	410.8	0.010	HOMO→L+2 (94)
4	25792	387.7	0.034	H-2→LUMO (28), H-2→L+1 (10), H-1→LUMO (42)
5	25897	386.1	0.034	H-2→LUMO (51), H-2→L+1 (18), H-1→LUMO (15)
6	25954	385.2	0.029	H-2→L+1 (12), H-1→LUMO (24), H-1→L+2 (39)
7	26440	378.2	0.029	H-2→L+1 (39), H-1→L+2 (36)
8	26517	377.1	0.038	H-2→L+2 (36), H-1→L+1 (41)
9	26992	370.4	0.006	H-2→L+2 (26), H-1→L+1 (17), HOMO→L+3 (35)
10	28122	355.5	0.067	H-2→L+2 (14), H-1→L+1 (13), HOMO→L+3 (57)
11	28940	345.5	0.006	H-1→L+3 (83)
12	28986	344.9	0.007	H-2→L+3 (79)
13	29417	339.9	0.029	H-3→LUMO (11), HOMO→L+4 (70)
14	29491	339.1	0.035	HOMO→L+5 (74)
15	29912	334.3	0.010	H-3→LUMO (58)
16	30083	332.4	0.029	H-4→LUMO (56), H-3→L+1 (13)
17	30467	328.2	0.043	H-3→L+1 (12), H-3→L+2 (53)
18	30559	327.2	0.120	H-3→L+1 (40), H-3→L+2 (20)
19	30668	326.0	0.057	H-5→LUMO (11), H-4->L+1 (45)
20	30723	325.4	0.020	H-2→L+5 (13), H-1→L+4 (56)

	ν(cm^{-1})	λ(nm)	f	Major contributions (%)
1	23723	421.5	0.030	HOMO→LUMO (86)
2	24754	403.9	0.028	HOMO→L+1 (84)
3	25494	392.2	0.022	H-1→LUMO (38), H-1→L+1 (55)
4	26066	383.6	0.033	H-1→LUMO (49), H-1→L+1 (36)
5	27677	361.3	0.006	HOMO→L+2 (24), HOMO→L+3 (67)
6	28039	356.6	0.013	H-4→LUMO (14), H-3→LUMO (20), H-2→LUMO (28)
7	28486	351.0	0.026	H-4→LUMO (10), HOMO→L+2 (52), HOMO→L+3 (12)
8	28705	348.3	0.000	H-1→L+2 (18), H-1→L+3 (61)
9	29109	343.5	0.023	H-4→L+1 (14), H-2→L+1 (29), H-1→L+2 (20), H-1→L+3 (10)
10	29523	338.7	0.074	H-3→LUMO (25), H-1→L+2 (24), HOMO→L+4 (17)
11	29694	336.7	0.016	H-4→LUMO (17), H-1→L+2 (23), HOMO→L+4 (36)
12	29810	335.4	0.028	H-3→LUMO (24), H-2→LUMO (33), HOMO→L+4 (25)
13	30428	328.6	0.113	H-3→L+1 (43), H-2→L+1 (28), H-1→L+4 (10)
14	30742	325.2	0.088	H-4→L+1 (15), H-2→L+1 (15), H-1→L+4 (56)
15	31156	320.9	0.277	H-4→LUMO (41), H-3→LUMO (18)
16	31355	318.9	0.111	H-4→L+1 (47), H-3→L+1 (21), H-1→L+4 (18)
17	32380	308.8	0.021	H-4→L+2 (17), H-3→L+2 (21), H-2→L+2 (53)
18	32902	303.9	0.027	H-3→L+3 (21), H-2→L+3 (58)
19	33490	298.5	0.009	H-3→L+2 (27), H-3→L+3 (14), H-2→L+2 (24), H-2→L+3 (11)

20	33690	296.8	0.044	H-3→L+2 (16), H-3→L+3 (13), H-3→L+4 (10), H-2→L+3 (16), H-2→L+4 (17)

Table S5 Computation of the triplet state positions for **1** and **2** in the gas phase.

Complex	$E(S_0)$ (a.u.)	$E(T_1)$ (a.u.)	Δ (a.u.)	Δ (eV)	position (nm)
1	-2577.90	-2577.79	0.102	2.77	447
2	-2098.78	-2098.69	0.092	2.50	495

Table S6 Key characteristics of the three-component WOLEDs with $Ir(ppy)_3$.

	$V_{turn\text{-}on}$ (V)	L_{max} (cd m^{-2}) @15 V	η_{ext} (%)[a]	η_L (cd A^{-1})[a]	η_P (lm W^{-1})[a]	CIE (x, y)[b]	CRI/CCT (K)
W4	4	26493	2.1 (4.4)	16.2 (5.4)	10.7 (4.6)	0.50, 0.37	64/2002
W5	4	27850	8.7 (5.6)	16.7 (5.6)	9.6 (5.4)	0.49, 0.38	69/2117
W6	4	35418	8.3 (5.6)	17 (5.6)	10.8 (4.8)	0.43, 0.39	79/2995

[a] Maximum values of the devices. Values in parentheses are the voltages at which they were obtained. [b] CIE coordinates (x, y) at 8 V.

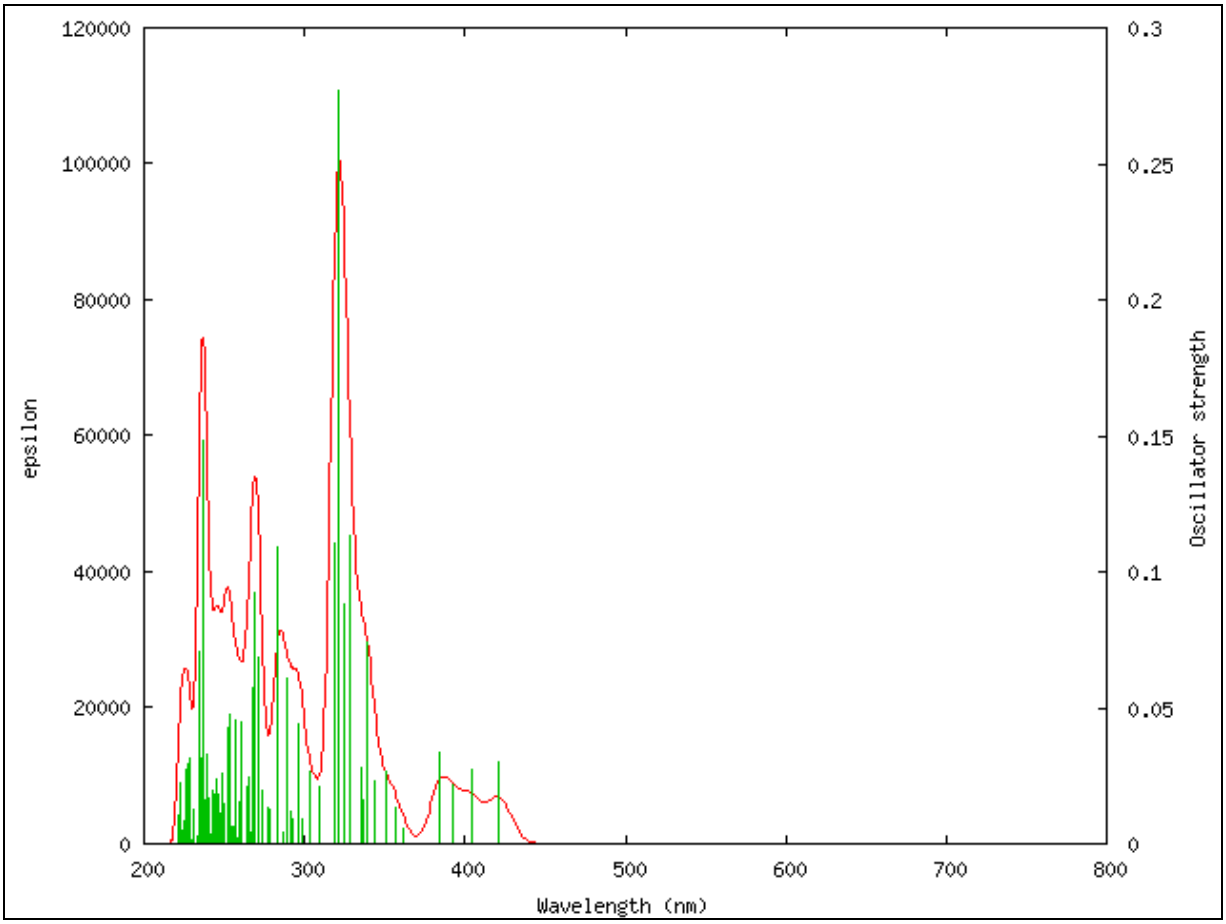

Fig. S1 Bar graph of the first 100 calculated electronic transitions for **1** (green) along with a spectrum generated by assigning a thickness to these lines (red). This graph does not include the vibronic progression.

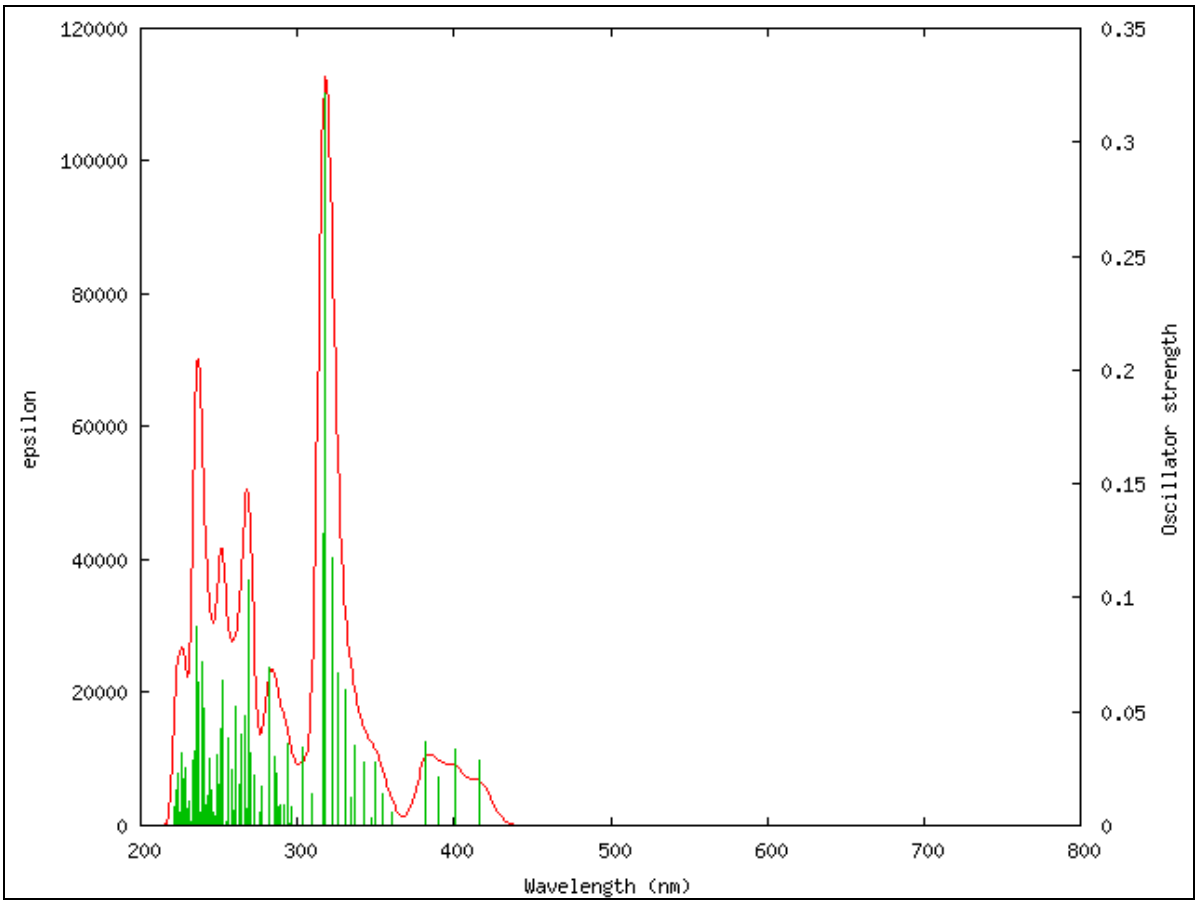

Fig. S2 Bar graph of the first 100 calculated electronic transitions for **2** (green) along with a spectrum generated by assigning a thickness to these lines (red). This graph does not include the vibronic progression.

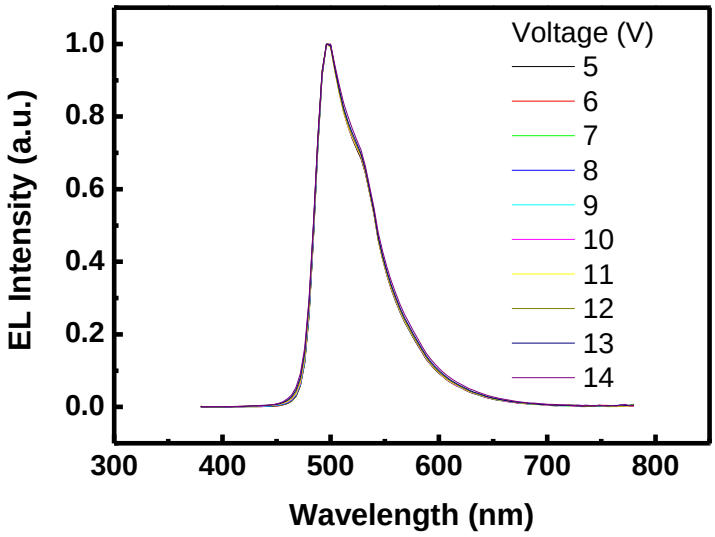

Fig. S3 The EL spectra for **G4** under different driving voltages.

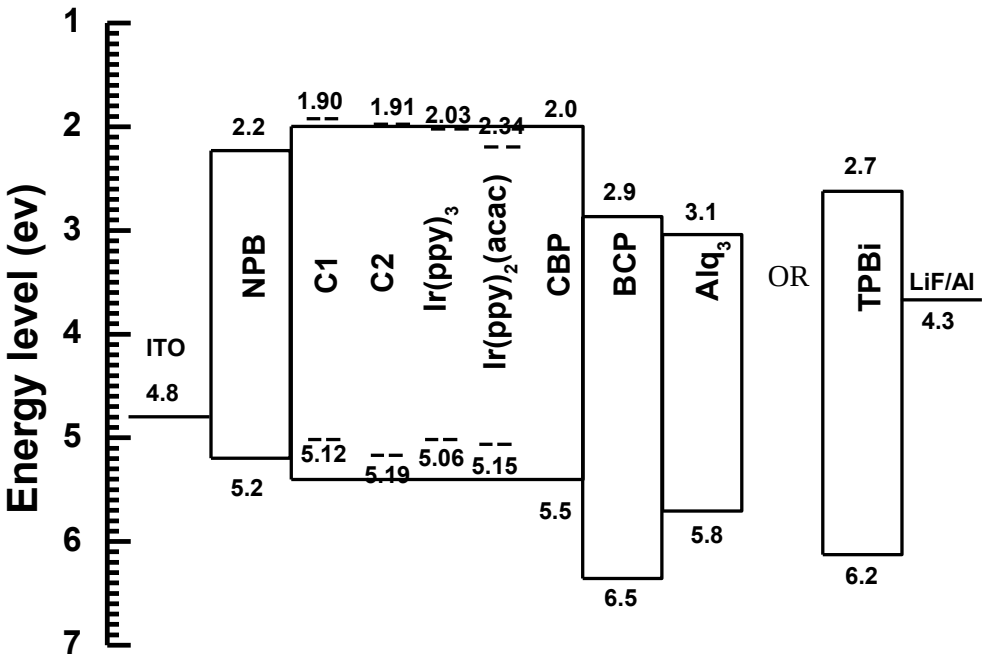

Fig. S4 Energy level diagram of OLEDs with BCP/Alq_3 or TPBi.

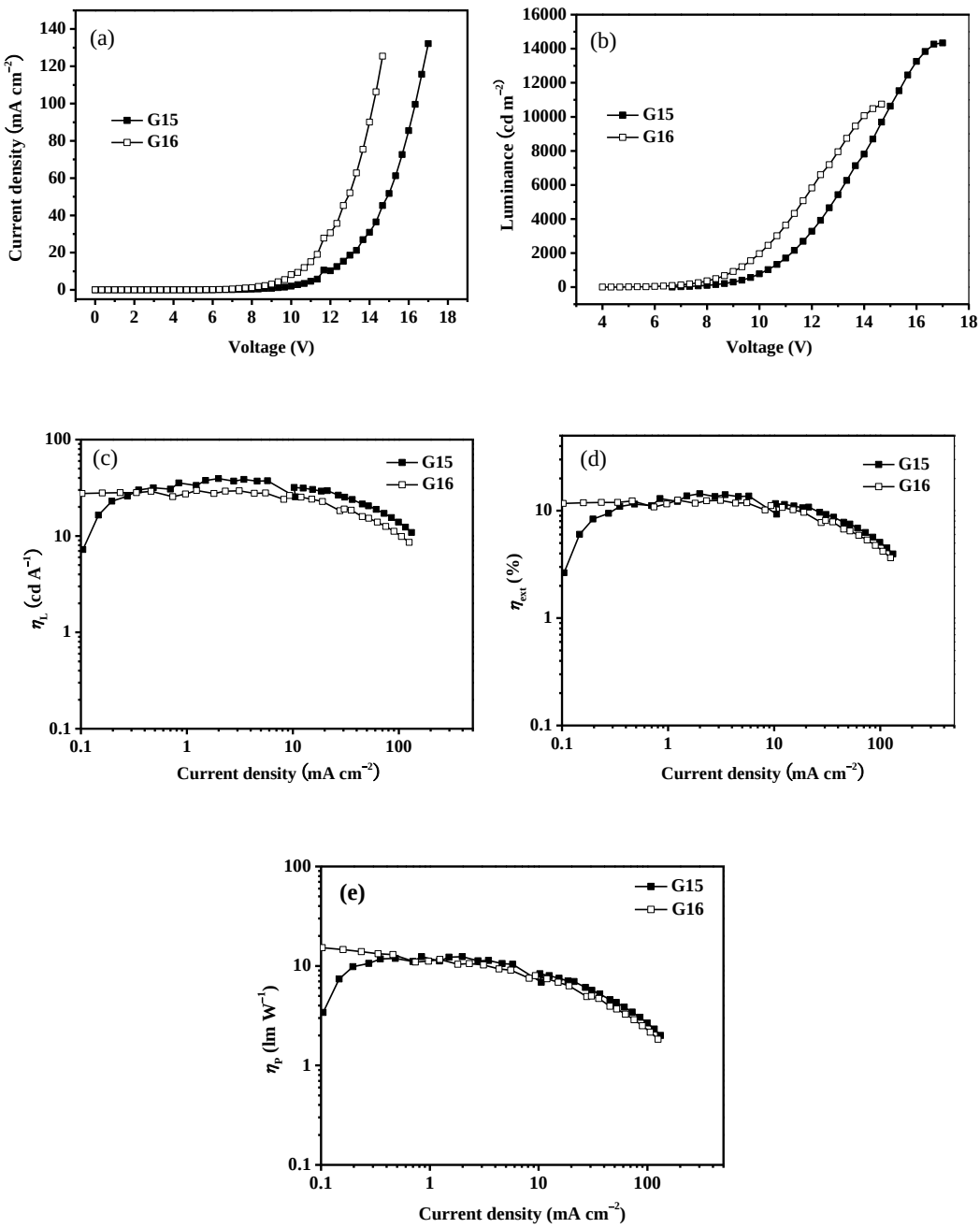

Fig. S5 Charts for the PLEDs **G15** and **G16** doped with **1** and **2**, respectively. (a) *J*–*V* curves; (b) *L*–*V* curves; (c) η_L–*J* curves; (d) η_{ext}–*J* curves and (e) η_P–*J* curves.

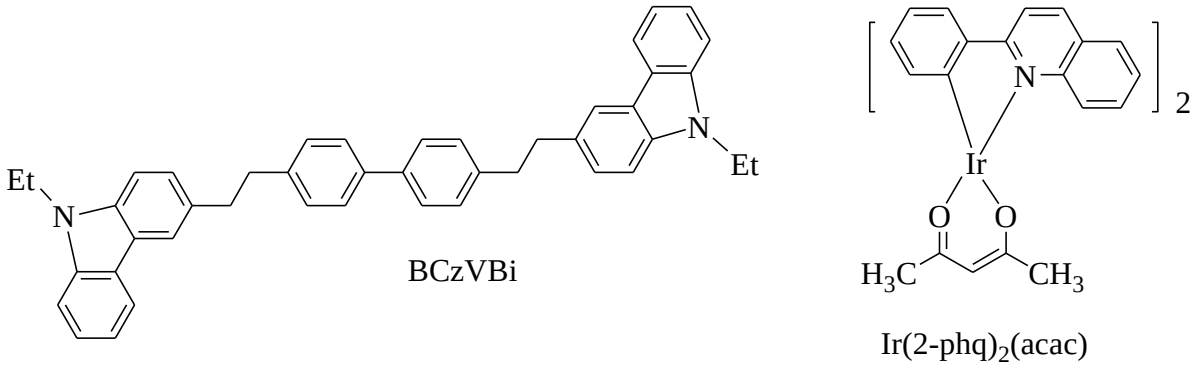

Fig. S6 Molecule structures of BCzVBi and Ir(2-phq)$_2$(acac).

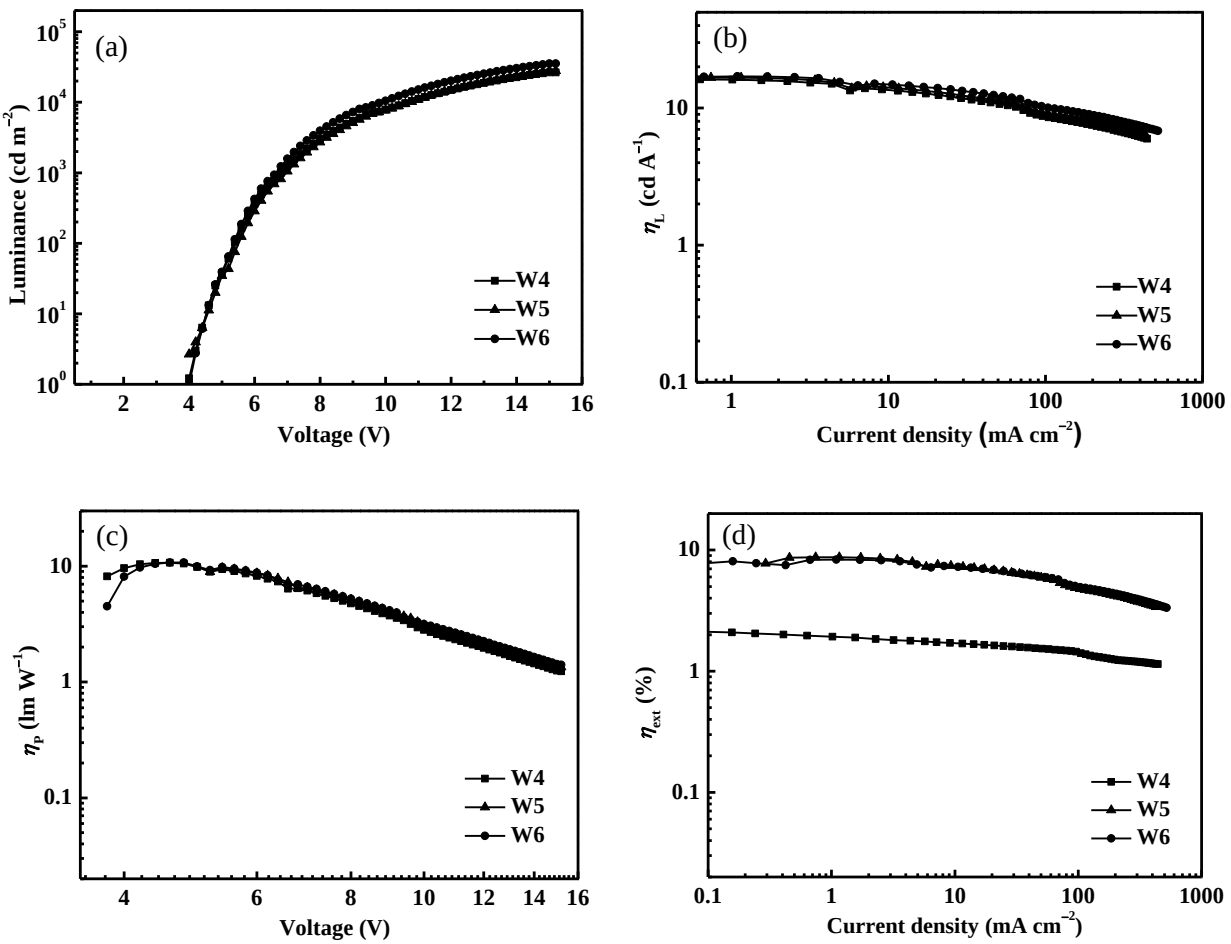

Fig. S7 Charts for the hybrid WOLEDs **W4**–**W6** doped with *fac*-Ir(ppy)$_3$, respectively. (a) L–V curves; (b) η_L–J curves; (c) η_P–V curves and (d) η_{ext}–J curves.

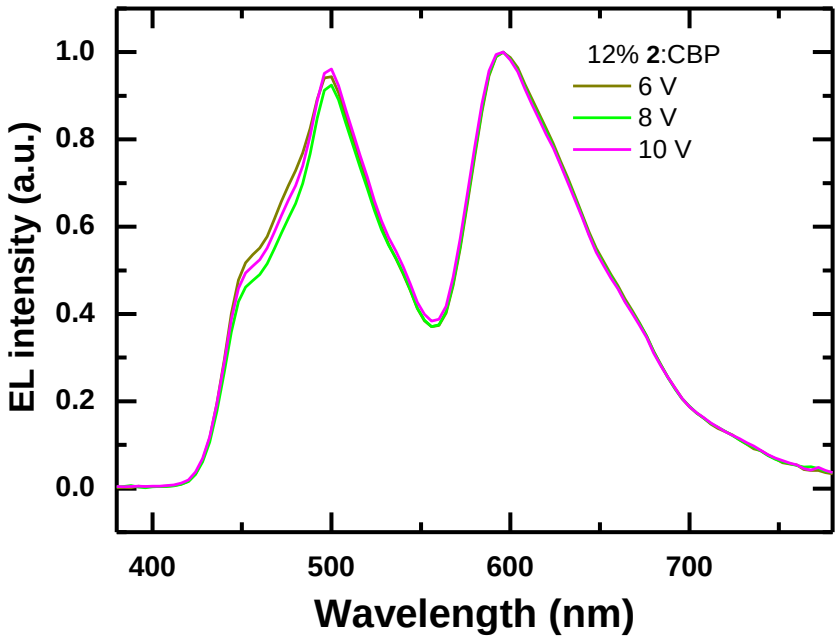

Fig. S8 EL spectra of the **2**-doped WOLED at different voltages.